Supporting Information

Bos et al. 10.1073/pnas.1213680110

SI Materials and Methods

Animals. *Wistar* rats were purchased from Janvier. Hb9::eGFP and *Slc12a5*$^{+/-}$ transgenic mice were kindly provided by T. Jessel (Columbia University, New York, NY) and E. Delpire (Vanderbilt University Medical Center, Nashville, TN), respectively. Animals were housed in a temperature-controlled animal care facility with a 12 h light–dark cycle. Generation and genotyping of the transgenic mice used have been described previously (1). We made all efforts to minimize animal suffering and the number of animals used. We performed experiments in accordance with French regulations (Ministry of Food, Agriculture and Fisheries, Division of Health and Protection of Animals). The local Direction of Veterinary Services and Ethical Committee (Marseille, Provence) delivered the appropriate licenses and approved the protocols, respectively.

Surgery. We anesthetized female rats (220–280 g) with a mixture of ketamine (60 mg/kg, i.p.; Imalgene; Merial) and medetomidine (0.25 mg/kg, i.p.; Domitor; Pfizer) and neonates by hypothermia. Amoxicillin, a long-lasting antibiotic, was administered immediately after anesthesia (150 mg/kg, s.c.; Clamoxyl LA; Pfizer). After laminectomy, we transected the spinal cord at the thoracic level (T8–T9). We treated sham-operated animals in the same way except for the spinal cord transection. Postsurgical care and treatments are described below. The surgery for transecting the spinal cord in neonates was similar to that described previously (2–4).

Postsurgical Treatments and Care of the Animals. After SCI in adult rats, we injected 5 mL of NaCl s.c., kept the rats warm until awakening, and placed some food with glucose in the cage. We administered buprenorphine to the rats every 8 h for 24 h (0.05 mg/kg, s.c.; Temgesic; Reckitt Benckiser Healthcare) and diluted DL-lysine acetylsalicylate in their drinking water for 3 d (200 mg in 150 mL of drinking water; Aspégic nourissons; Sanofi Aventis). Twice a day, we manually emptied their bladders until recovery of the urinary function, checked their temperature and hydration, and observed any clinical sign of pain or infection. No urinary infection occurred. We killed rats presenting a more than 20% decrease in body weight, a temperature under 35 °C, or signs of autophagia with a lethal dose of pentobarbital.

Chronic Pharmacological Treatment. We activated 5-HT$_2$Rs in animals with a SCI at birth by daily i.p. administration of the 5-HT$_2$R agonist DOI, from P4 to P6–P7 [0.15 mg/kg DOI diluted in 50 μL of NaCl (2, 4)]. Sham-treated animals were injected with 50 μL of NaCl only.

Western Blot. We euthanized animals by decapitation and quickly dissected out and froze T8-sacral parts of the spinal cords. For each sample, two spinal cords were pooled. For cytoplasmic and membrane fractions, we homogenized samples in cold lysis buffer B (described below) without detergent and centrifuged them first at 7,000 × *g* for 5 min and then at 18,000 × *g* for 70 min at 4 °C. We collected pellets (membrane-enriched fractions) in lysis buffer A and supernatants (cytoplasmic fractions). We determined supernatant protein concentrations using a detergent-compatible protein assay (Bio-Rad). We then immunoprecipitated KCC2 (described below), separated samples in 6% (vol/vol) SDS/PAGE from 40% Acryl/Bisacrylamide (29/1) commercial solution, and transferred them to a PVDF membrane. After blockade in Tris-buffered saline–5% nonfat dry milk, we exposed membranes overnight at 4 °C to a polyclonal rabbit KCC2-specific antibody diluted at 1:700 (Millipore) in the blocking solution. The specificity of the KCC2 antibody to KCC2 is confirmed by the lower intensity of the signal in *Slc12a5*$^{+/-}$ and *Slc12a5*$^{-/-}$ mice (5). We used an ImmunoPure goat HRP-conjugated rabbit-specific antibody (1:120,000 in blocking solution; 1 h at 22 °C; Pierce Biotech) for chemiluminescent detection (Millipore). Signal intensities were measured with the image analysis software Quantity-One (Bio-Rad).

Composition of lysis buffer A. The composition of buffer A was 1% Igepal CA-630, 0.1% SDS, 10 mM sodium vanadate, 10 mM sodium fluoride, 10 mM sodium pyrophosphate, 10 mM iodoacetamide, and a mixture of protease inhibitors (CompleteMini; Roche Diagnostics).

Composition of lysis buffer B. The composition of buffer B was sucrose 320 mM in Tris-HCl (pH 7.5), 10 mM sodium vanadate, 10 mM sodium fluoride, 10 mM sodium pyrophosphate, 10 mM iodoacetamide, and a mixture of protease inhibitors.

KCC2 immunoprecipitation. We incubated the same amount of protein with an affinity-purified rabbit KCC2-specific polyclonal antibody (Millipore) for 4 h at 4 °C and precipitated the protein–antibody complexes with PureProteome protein G magnetic beads (Millipore). After several washes in lysis buffer, beads were resuspended in SDS sample buffer.

Immunohistochemistry and Quantification of KCC2 Labeling. For immunohistochemistry, we anesthetized the animals at P7 by hypothermia, and killed them by decapitation (n = 3 in each group). We rapidly excised the lumbar spinal cord, immersed it for 1 h in 20% sucrose, and embedded it in capsules filled with Tissutech (Sakura) quickly frozen by immersion in ethanol 100% kept at –80 °C. We cut transverse spinal cord sections (20 μm thick) with a cryostat (Microm) and mounted them onto gelatinized slides. We immersed section in 2% paraformaldehyde in 0.15 M PBS (pH 7.4) for 30 min and rinsed in PBS. We incubated sections overnight at 4 °C in a mixture of affinity-purified rabbit KCC2-specific polyclonal antibody (1:200; Millipore) and GlyR monoclonal antibody (mAb2b; 1:100; Synaptic Systems). We then revealed the labeling with a mixture of donkey Cy3-conjugated rabbit-specific antibody (1:500; Jackson Immunoresearch) and donkey AlexaFluor 488–conjugated mouse-specific antibody (1:800, Molecular Probes; 1 h at 22 °C) and mounted coverslips with a gelatinous aqueous medium. We analyzed the patterns of immunolabeling by means of a laser scanning confocal microscope (SM 510 META; Zeiss) at low (20×) or high magnification ([63× 1.4 (NA) oil immersion objective; Plan Apochromat].

Triple-fluorescent labelings were captured using frame-channel mode to avoid any cross-talk between the channels. Each optical section resulted from two scanning averages. Excitation of the fluorochromes was performed with a diode laser set at 405 nm to detect FB, an argon ion laser set at 488 nm, and a helium/neon laser set at 575 nm. At high magnification, we only scanned FB-retrogradely labeled TS motoneurons with visible nuclei, and for each soma, we digitized stacks of 1-μm-thick optical sections. Because the developmental up-regulation of GlyR is not affected by neonatal transaction (2), we used the GlyR immunolabeling to delimit the somatic membrane of the motoneurons in sham-operated, transected, and DOI-treated transected animals, respectively. We overlaid the internal and external borders and digitized intensity measurements of KCC2 labeling using the Fluoview software (Version 5; Olympus). To quantify KCC2 labeling in the dendrites, we framed a zone of the white matter underneath the IX layers of Rexed laminae. We used the nonparametric one-way ANOVA

(Kruskal–Wallis) with a Dunn's post test for multiple comparisons between sham animals and SCI and/or SCI-pharmacologically treated rats.

Motoneuron Culture and Immunocytochemistry. Hb9::GFP transgenic mice were maintained as hemizygotes by crossing with nontransgenic female mice. Mice were housed in a conventional dark/light cycle (dark 1100 hours to 0900 hours) and positive vaginal plugs at 0900 hours were recorded as embryonic day (E)0. Motoneurons were isolated from E12 spinal cords essentially as described previously (6, 7). Motoneurons were seeded at a density of about 5.000 cells per well in four-well plates previously treated with polyornithine (Life Technologies) and laminin (Becton Dickinson). Motoneurons were cultured in Neurobasal medium supplemented with 2% (vol/vol) horse serum, 25 μM L-glutamate, 25 μM β-mercaptoethanol, 0.5 mM L-glutamine, 2% (vol/vol) B-27 (all from Life Technologies), and the neurotrophic factors BDNF (1 ng/mL; R&D Systems), ciliary neurotrophic factor (CNTF) (10 ng/mL; R&D Systems), and glial cell line-derived neurotrophic factor (GDNF) (100 pg/mL; Sigma). Half of the culture medium was replaced every 2 d.

At 13 or 14 DIV, cultures were incubated with TCB-2 or mock for 30 min at 37 °C in an incubator containing 5% CO_2 in a humidified air atmosphere. Cultures were fixed for 15 min by adding an equal volume of 7.4% (vol/vol) formaldehyde in PBS, washed and blocked in buffer containing PBS, 0.1% Triton X-100, 1% BSA, and 5% goat serum. Coverslips were incubated overnight at 4 °C with rabbit polyclonal anti-KCC2 antibodies (Millipore) at 1:300 in blocking buffer, washed with PBS, and incubated for 1 h with Cy3-conjugated anti-rabbit antibodies (Jackson Immunoresearch) diluted in blocking buffer. Coverslips were mounted in Vectashield/DAPI solution (Vector Labs) and examined with a confocal fluorescence microscope (60× oil objective; Fluoview; Olympus). Thirty-four randomly chosen cells per condition from two independent experimental series were imaged at 3× magnification using identical settings for laser power, photomultipliers, electronic gain, and offset. For each cell, plasma membrane and cytosol were manually delimited and fluorescence intensities in both areas were quantified using the Neuron J plugin of the ImageJ software (National Institutes of Health). The individuals performing data analysis were blind to the conditions of motoneurons.

In Vitro Electrophysiological Recordings. The aCSF used for perfusion was composed of 130 mM NaCl, 4 mM KCl, 3.75 mM $CaCl_2$, 1.3 mM $MgSO_4$, 0.58 mM NaH_2PO_4, 25 mM $NaHCO_3$, and 10 mM glucose and was oxygenated with 95% O_2 and 5% CO_2 (pH 7.4; temperature 24–25 °C).

Intracellular recordings. We measured the effects of various pharmacological compounds on the reversal potentials of IPSPs (3) (E_{IPSP}) from the spinal cord of intact and cord-transected rats (P5–P7). We also measured E_{IPSP} 4–6 d after transection or sham surgery performed at P0. After removing the pia, we recorded lumbar motoneurons intracellularly using glass microelectrodes filled with 2 M K-acetate (90- to 150-MΩ resistance). We recorded intracellular potentials in the discontinuous current–clamp (DCC) mode (Axoclamp 2B amplifier; Digidata 1200 interface; pClamp9 software; Axon Instruments). We considered only neurons exhibiting a stable (>15 min) resting membrane potential for analysis. We identified motoneurons in the L4–L5 segments by their antidromic response to ventral root stimulation. We used glass suction electrodes to stimulate the ipsilateral ventral funiculus at the L2–L3 level. Such stimulations induced $GABA_A$ R– and GlyR-mediated IPSPs (3, 8, 9) in the presence of 2-amino-5-phosphonovaleric acid (AP5) (50–100 μM) and 6-cyano-7-nitroquin-oxaline-2,3-dione (CNQX) (10 μM). We recorded IPSPs at various holding potentials (500-ms-long current pulses) and collected at least 20 values for each motoneuron. We measured and plotted amplitudes of IPSPs against holding potentials and obtained E_{IPSP} from the regression line (Prism Version 5; Graphpad).

Quantification of polysynaptic responses. We placed monopolar stainless steel electrodes in contact with the spinal roots and insulated them with Vaseline for stimulation and recording (P5–P7). We recorded L4–L5 ventral roots discharges by means of an AC-coupled amplifier (bandwidth: 70 Hz to 3 kHz) in response to the stimulation of the homonymous dorsal root (0.3 ms). Stimulations were delivered at supramaximal intensity every 60 s to avoid the synaptic depression described in this preparation. Once the signal was stable for at least 20 min, we added the pharmacological compound to be tested to the perfusion liquid for 20–30 min. We rectified signals and measured the areas under the curve from 3 to 100 ms after the onset of the monosynaptic signal (pClamp9 software). The effect of the drug was considered 20 min following bath application of the compound.

Measurement of RDD in vitro. We delivered supramaximal electrical stimulations (0.3-ms duration) to dorsal roots. We measured the amplitude of the monosynaptic response between the first positive and negative peaks. We delivered 15 stimulations at various frequencies (30 s between each series). We normalized the amplitude of responses (the first three discarded) to the controls evoked at 30-s intervals (mean of five pulses). We took into account at least three series of stimulations before and 20–30 min after the application of the compound.

Fictive locomotion. The coordination between opposite L3 ventral root bursts was investigated during fictive locomotion in six transected animals (4) (P5, $n = 3$; P6, $n = 3$). Fictive locomotion was elicited by bath application of *N*-methyl-D, L-aspartate (NMA) (12–16 μM). Analyses consisted in rectifying and integrating the recordings (time constant of 25 ms). A threshold function was used to determine bursts onset and termination. The threshold was usually set to ~30% of the peak value. The duration of motor bursts was measured, and the middle of bursts was considered to calculate the period (defined as the time between the midpoint of two consecutive bursts) and the phase relationships between the left and right bursts (defined as the time between the midpoint of a burst and that of the next burst in the contralateral root, divided by the period of the ongoing cycle). The coordination was evaluated by means of cross-correlation analysis (pClamp9 software; Axon Instruments). Phase data were multiplied by 360° to be analyzed by means of circular statistics (Oriana; Kovach Computing Services).

In Vivo Electrophysiological Recordings (H Reflex). We repeated a series of measurements throughout the experiment. First, we stimulated the tibial nerve for 0.2 ms at 0.2 Hz with increasing current intensities (until M_{max} was stabilized) and determined the intensity necessary to get a maximal H response. Then, we used this intensity for trains of 20 stimulations at 0.1, 0.5, 1, 2, and 5 Hz to measure the RDD, with at least 1-min intervals between each train of stimulations so that a whole series of measurements lasted about 15min. We added one third of the initial dose of anesthesia every 30 min and maintained the rat temperature around 37 °C. To determine the level of RDD at the different frequencies, we discarded responses to the first three stimulations necessary for the depression to occur and expressed all of the responses as percentages relative to the mean response at 0.2 Hz in the same series of measurements.

We injected the drug or its vehicle after two stable series of measurements and carried on measuring current–voltage (I/V) curves and RDD for 3 h.

Drugs. We purchased DOI hydrochloride, ketanserin tartrate, VU0240551, PDBu, α-methyl 5-HT, NMA, strychnine, and picrotoxin from Sigma. We purchased TCB-2, MDL11,939, SB206553 hydrochloride, chelerythrine chloride, Gö6976, and FR236924 (DCP-LA) from Tocris. DL-AP5 and CNQX were purchased from Abcam. All compounds were prepared in aCSF except

VU0240551, PDBu, α-methyl 5-HT, MDL11,939, SB206553 hydrochloride, chelerythrine chloride, Gö6976, and FR236924, which were diluted in DMSO (0.1% final concentration).

Statistical Analyses. Group measurements are expressed as means ± SEM. We used *t* tests to compare two groups and one- or two-way ANOVA to compare more than two groups, or corresponding nonparametric analyses when data were not normally distributed or when small samples (<20) were analyzed (Prism 5 software; Graphpad). Nonlinear regressions were performed to compare the levels of H-reflex depression at all stimulation frequencies tested in different groups. A logarithmic transformation of frequency values was also performed to enable linear regression analyses and comparison of slopes. Statistical tests used in each case are given in figure legends. The level of significance was set at $P < 0.05$.

1. Jiang Z, Carlin KP, Brownstone RM (1999) An in vitro functionally mature mouse spinal cord preparation for the study of spinal motor networks. *Brain Res* 816(2):493–499.
2. Sadlaoud K, et al. (2010) Differential plasticity of the GABAergic and glycinergic synaptic transmission to rat lumbar motoneurons after spinal cord injury. *J Neurosci* 30(9):3358–3369.
3. Jean-Xavier C, Pflieger JF, Liabeuf S, Vinay L (2006) Inhibitory postsynaptic potentials in lumbar motoneurons remain depolarizing after neonatal spinal cord transection in the rat. *J Neurophysiol* 96(5):2274–2281.
4. Norreel JC, et al. (2003) Reversible disorganization of the locomotor pattern after neonatal spinal cord transection in the rat. *J Neurosci* 23(5):1924–1932.
5. Stil A, et al. (2011) Contribution of the potassium-chloride co-transporter KCC2 to the modulation of lumbar spinal networks in mice. *Eur J Neurosci* 33(7):1212–1222.
6. Raoul C, et al. (2006) Chronic activation in presymptomatic amyotrophic lateral sclerosis (ALS) mice of a feedback loop involving Fas, Daxx, and FasL. *Proc Natl Acad Sci USA* 103(15):6007–6012.
7. Arce V, et al. (1999) Cardiotrophin-1 requires LIFRbeta to promote survival of mouse motoneurons purified by a novel technique. *J Neurosci Res* 55(1):119–126.
8. Bos R, Brocard F, Vinay L (2011) Primary afferent terminals acting as excitatory interneurons contribute to spontaneous motor activities in the immature spinal cord. *J Neurosci* 31(28): 10184–10188.
9. Boulenguez P, et al. (2010) Down-regulation of the potassium-chloride cotransporter KCC2 contributes to spasticity after spinal cord injury. *Nat Med* 16(3):302–307.

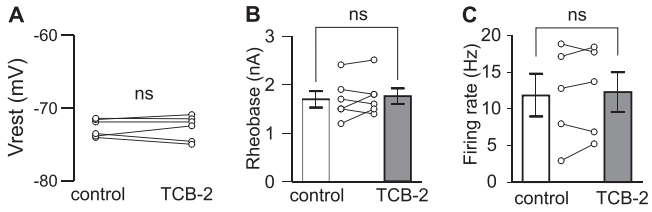

Fig. S1. TCB-2 has no effect on several electrical properties of motoneurons. (*A*) V_{rest} of six motoneurons (control rats; P5–P7) before and 20–30 min after starting bath application of TCB-2 (0.1 μM diluted in aCSF). (*B* and *C*) TCB-2 has a significant effect neither on the rheobase (defined as the minimum current required to induce action potential during a 500 ms pulse; $n = 5$) (*B*) nor on the firing rate ($n = 5$) (*C*). The firing rate was recorded at 1.5-twofold the rheobase in the both conditions. ns, $P > 0.05$ (Wilcoxon paired test).

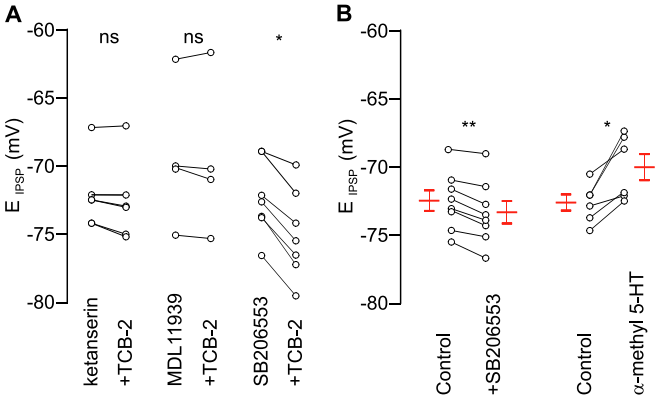

Fig. S2. Relative effects of blocking or activating 5-HT_{2A}R and 5-$HT_{2B/C}$R on E_{IPSP}. (*A*) Preincubation during 30 min of the 5-HT_2R antagonist ketanserin (1 μM; $n = 4$) or the more specific 5-HT_{2A}R antagonist MDL11,939 (2 μM; $n = 4$) prevented the hyperpolarizing effect of TCB-2 (0.1 μM) on E_{IPSP}. The latter compound had no effect on E_{IPSP} (−70.6 and −70.8 mV in control and under MDL11,939, respectively; $n = 4$). TCB-2 (0.1 μM) still induced a hyperpolarizing shift of E_{IPSP} in the presence of the 5-HT_{2B-C}R antagonist SB206553 (3–5 μM; $n = 6$). (*B*) Hyperpolarizing effect of the 5-$HT_{2B/2C}$R antagonist SB206553 (3–5 μM) on E_{IPSP} in motoneurons recorded from control rats (P5–P7; $n = 8$). E_{IPSP} was significantly more depolarized after application of the 5-$HT_{2B/2C}$R agonist α-methyl 5-HT (0.5–5 μM) compared with control (P5–P6 rats; $n = 6$). These results suggest that 5-HT_{2B}R and/or 5-HT_{2C}R exert a depolarizing action on E_{IPSP}. ns, $P > 0.05$; $*P < 0.05$; $**P < 0.01$ (Wilcoxon paired test).

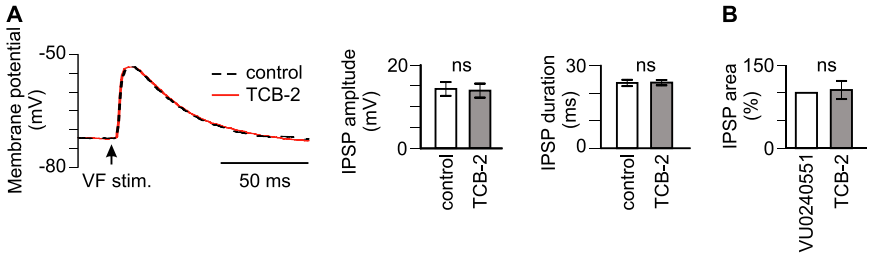

Fig. S3. TCB-2 has no effect on IPSP kinetics. (*A*) IPSP recorded by means of a microelectrode filled with KCl (2 M) to load the cell with Cl^- and, thereby, shift E_{IPSP}. The IPSP was quite similar before and after adding TCB-2 (0.1 μM). No significant difference was observed on both the amplitude (n = 6) (*Center*) and the duration (n = 6) (*Right*) of IPSPs from newborn rats (P4–P5). (*B*) The area of IPSPs was measured at V_{rest} before and after adding TCB-2 in the continuous presence of VU0240551 at 25 μM (P5–P6 rats; n = 11). ns, $P > 0.05$ (Wilcoxon paired test).

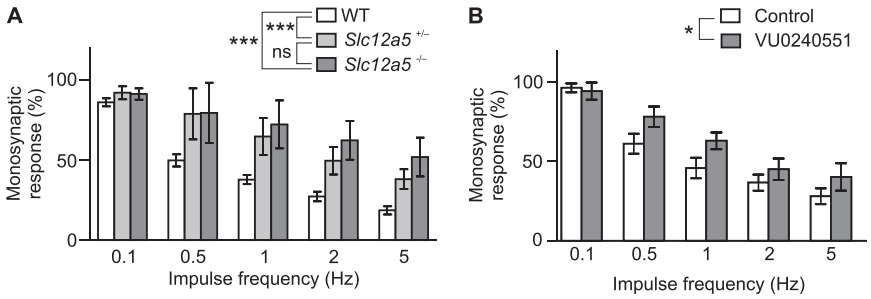

Fig. S4. RDD of the monosynaptic reflex in vitro is reduced when KCC2 function is genetically or pharmacologically reduced. (*A*) To investigate the role of KCC2 in this property of spinal cord reflexes, we used *Slc12a5*$^{+/-}$ mice (n = 7) and *Slc12a5*$^{-/-}$ mice (1) (n = 4), which retain ∼50% and 10% of normal KCC2 protein amounts in the spinal cord, respectively (2). RDD was significantly smaller in both types of mice compared with wild-type mice (n = 9), confirming that KCC2 cotransporters play a key role in the depression of the response. (*B*) The specific blockage of KCC2 by VU0240551 (25 μM; P5–P6 rats; n = 4) significantly decreases the RDD of the monosynaptic reflex. ns, $P > 0.05$; *$P < 0.05$; ***$P < 0.001$ (one-phase exponential decay regression).

1. Stil A, et al. (2011) Contribution of the potassium-chloride co-transporter KCC2 to the modulation of lumbar spinal networks in mice. *Eur J Neurosci* 33(7):1212–1222.
2. Woo NS, et al. (2002) Hyperexcitability and epilepsy associated with disruption of the mouse neuronal-specific K-Cl cotransporter gene. *Hippocampus* 12(2):258–268.

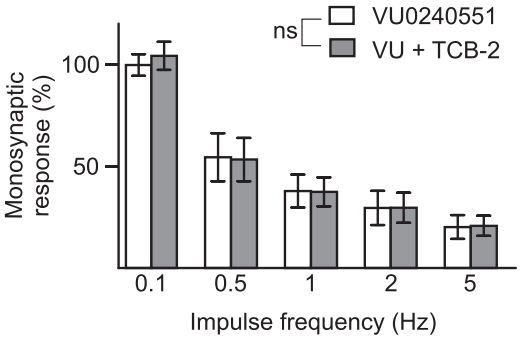

Fig. S5. Blocking KCC2 prevents the effect of TCB-2 on the RDD of the monosynaptic reflex in vitro. TCB-2 (0.1 μM) did not increase the RDD of the monosynaptic response in the continuous presence of the specific blocker of KCC2 (VU0240551; 25 μM; P5–P6 rats; n = 4). ns, $P > 0.05$ (Wilcoxon paired test).

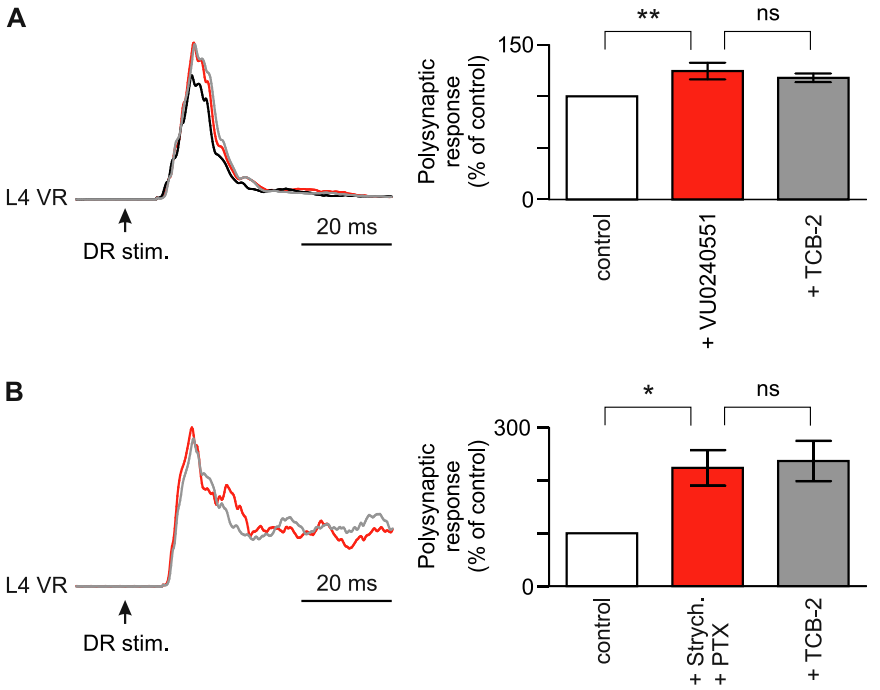

Fig. S6. TCB-2 reduces polysynaptic ventral root responses through a modulation of chloride homeostasis. (*A*) The specific blocker of KCC2 (VU0240551; 25 μM) significantly increased the polysynaptic ventral root responses and prevented the effect of TCB-2 on the polysynaptic response (P5 rats). ns, $P > 0.05$; $^{**}P < 0.01$ (Kruskal–Wallis test with Dunn's post test; $n = 4$ in each group). (*B*) The polysynaptic ventral root responses (rectified averaged signals) was significantly increased in presence of the GlyR and GABA receptor antagonists [strychnine and picrotoxin (PTX), respectively] compared with control conditions (P5–P6 rats). The decrease of the polysynaptic response by TCB-2 (0.1 μM) (Fig. 4) was prevented in the continuous presence of strychnine and PTX. ns, $P > 0.05$; $^{*}P < 0.05$ (Kruskal–Wallis test with Dunn's post test; $n = 4$ in each group).

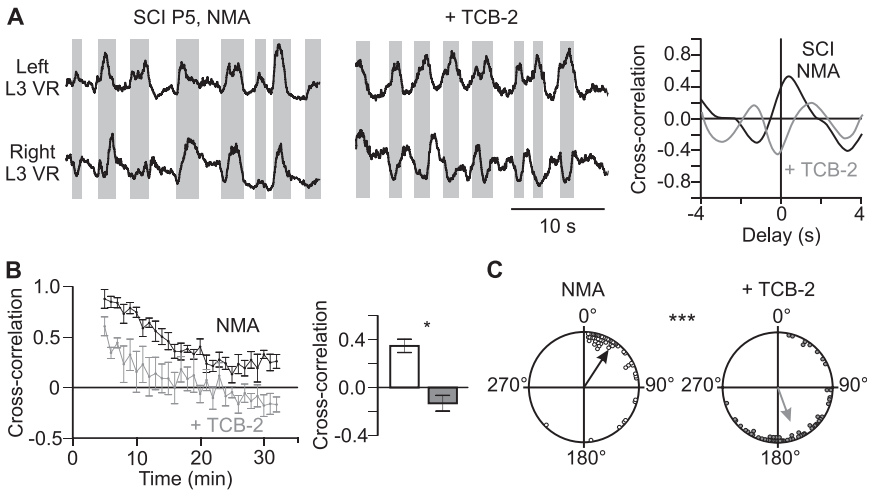

Fig. S7. Activation of 5-HT_{2A}Rs in vitro restores the left–right alternating locomotor pattern after neonatal spinal cord transection. (*A*) Integrated recordings from the left and right L3 ventral roots (VR) at P5 in the presence of NMA alone (16 μM) (*Left*) or together with 5-HT_{2A}R agonist TCB-2 (0.1 μM) (*Center*). Gray areas indicate the bursts occurring in the left L3 VR. Cross-correlograms between the two VR signals computed from 10 min of activity induced by NMA alone (black line) or NMA and TCB-2 (gray line). (*B*) Time course of the changes of cross-correlation coefficient in six transected rats in NMA alone (10–16 μM, black plot) or NMA and TCB-2 (0.1 μM, gray plot). Mean cross-correlation coefficient (*Right*) between left and right ventral root activities computed when activities were stable in both conditions (5–10 min). $^{*}P < 0.05$ (Wilcoxon paired test; $n = 6$). (*C*) Distribution of phase relationships between left and right ventral root bursts in NMA alone (*Left*) and NMA plus TCB-2 (*Right*) in all of the spinal animals (P5–P6; $n = 6$).

Table S1. Agonists/antagonists of 5-HT$_2$R and their receptor-binding affinity

		K_i (nM)		
Agonists [ref(s).]	Antagonists [ref(s).]	5-HT$_{2A}$R	5-HT$_{2B}$R	5-HT$_{2C}$R
DOI (1–3)		0.7	27.54	9.3
TCB-2 (4)		0.73	None	None
α-Methyl 5-HT (2, 3, 5)		127.05	10.47	2.69
	Ketanserin (3, 6)	1.49	740	59
	MDL11,939 (3)	26.3	3310	263.06
	SB206553 (3, 7)	2,300	5.5	3.2

1. Egan C, et al. (2000) Agonist high and low affinity state ratios predict drug intrinsic activity and a revised ternary complex mechanism at serotonin 5-HT(2A) and 5-HT(2C) receptors. *Synapse* 35(2):144–150.
2. Boess FG, Martin IL (1994) Molecular biology of 5-HT receptors. *Neuropharmacology* 33(3-4):275–317.
3. Knight AR, et al. (2004) Pharmacological characterisation of the agonist radioligand binding site of 5-HT(2A), 5-HT(2B) and 5-HT(2C) receptors. *Naunyn Schmiedebergs Arch Pharmacol* 370(2):114–123.
4. McLean TH, et al. (2006) 1-Aminomethylbenzocycloalkanes: Conformationally restricted hallucinogenic phenethylamine analogues as functionally selective 5-HT2A receptor agonists. *J Med Chem* 49(19):5794–5803.
5. Engel G, Göthert M, Hoyer D, Schlicker E, Hillenbrand K (1986) Identity of inhibitory presynaptic 5-hydroxytryptamine (5-HT) autoreceptors in the rat brain cortex with 5-HT1B binding sites. *Naunyn Schmiedebergs Arch Pharmacol* 332(1):1–7.
6. Aloyo VJ, Harvey JA (2000) Antagonist binding at 5-HT(2A) and 5-HT(2C) receptors in the rabbit: High correlation with the profile for the human receptors. *Eur J Pharmacol* 406(2): 163–169.
7. Cussac D, et al. (2002) Characterization of phospholipase C activity at h5-HT2C compared with h5-HT2B receptors: Influence of novel ligands upon membrane-bound levels of [3H] phosphatidylinositols. *Naunyn Schmiedebergs Arch Pharmacol* 365(3):242–252.

Table S2. Characteristics of the M and H waves before and 7 min after injection of TCB-2

	Before TCB-2 (mean ± SEM)	After TCB-2 (mean ± SEM)	Wilcoxon paired test (*P*)*
Threshold (mA)	2.35 ± 0.86	2.85 ± 1.09	0.25
M_{max} (mV)	3.42 ± 0.61	2.83 ± 0 0.33	0.13
I-M_{max} (mA)	4.10 ± 1.21	4.25 ± 1.40	0.75
H_{max} (mV)	1.90 ± 0.46	0.84 ± 0.14	0.13
I-H_{max}	3.26 ± 1.22	4.30 ± 1.39	0.20
H_{max}/M_{max}	0.55 ± 0.09	0.32 ± 0.09	0.13

The TCB-2 injection was 0.3 mg/kg, i.p.

*None of the paired comparison was significant ($P > 0.05$; $n = 4$).